

Tunable delay control of entangled photons based on dispersion cancellation

Ogaga D. Odele,¹ Joseph M. Lukens,¹ Jose A. Jaramillo-Villegas,^{1,2}
Carsten Langrock,³ Martin M. Fejer,³ Daniel E. Leaird,¹ and
Andrew M. Weiner^{1,*}

¹*School of Electrical and Computer Engineering, Purdue University, West Lafayette, Indiana 47906, USA*

²*Facultad de Ingenierías, Universidad Tecnológica de Pereira, Pereira, Risaralda 660003, Colombia*

³*E. L. Ginzton Laboratory, Stanford University, Stanford, California 94305, USA*

*amw@purdue.edu

Abstract: We propose and demonstrate a novel approach for controlling the temporal position of the biphoton correlation function using pump frequency tuning and dispersion cancellation; precise waveguide engineering enables biphoton generation at different pump frequencies while the idea of nonlocal dispersion cancellation is used to create the relative signal-idler delay and simultaneously prevents broadening of their correlation. Experimental results for delay shifts up to ± 15 times the correlation width are shown along with discussions of the performance metrics of this approach.

© 2015 Optical Society of America

OCIS codes: (270.0270) Quantum optics; (190.4410) Nonlinear optics, parametric processes; (260.2030) Dispersion; (320.5540) Pulse shaping.

References and links

1. N. Gisin, G. Ribordy, W. Tittel, and H. Zbinden, "Quantum cryptography," *Rev. Mod. Phys.* **74**, 145–195 (2002).
2. H.-K. Lo, M. Curty, and K. Tamaki, "Secure quantum key distribution," *Nat. Photon.* **8**, 595–604 (2014).
3. C. H. Bennett and D. P. DiVincenzo, "Quantum information and computation," *Nature* **404**, 247–255 (2000).
4. T. D. Ladd, F. Jelezko, R. Laflamme, Y. Nakamura, C. Monroe, and J. L. O'Brien, "Quantum computers," *Nature* **464**, 45–53 (2010).
5. C. H. Bennett, G. Brassard, C. Crépeau, R. Jozsa, A. Peres, and W. K. Wootters, "Teleporting an unknown quantum state via dual classical and Einstein-Podolsky-Rosen channels," *Phys. Rev. Lett.* **70**, 1895–1899 (1993).
6. J. Yin, J.-G. Ren, H. Lu, Y. Cao, H.-L. Yong, Y.-P. Wu, C. Liu, S.-K. Liao, F. Zhou, Y. Jiang, X.-D. Cai, P. Xu, G.-S. Pan, J.-J. Jia, Y.-M. Huang, H. Yin, J.-Y. Wang, Y.-A. Chen, C.-Z. Peng, and J.-W. Pan, "Quantum teleportation and entanglement distribution over 100-kilometre free-space channels," *Nature* **488**, 185–188 (2012).
7. X.-S. Ma, T. Herbst, T. Scheidl, D. Wang, S. Kropatschek, W. Naylor, B. Wittmann, A. Mech, J. Kofler, E. Anisimova, V. Makarov, T. Jennewein, R. Ursin, and A. Zeilinger, "Quantum teleportation over 143 kilometres using active feed-forward," *Nature* **489**, 269–273 (2012).
8. V. Giovannetti, S. Lloyd, and L. Maccone, "Quantum-enhanced positioning and clock synchronization," *Nature* **412**, 417–419 (2001).
9. V. Giovannetti, S. Lloyd, and L. Maccone, "Advances in quantum metrology," *Nat. Photon.* **5**, 222–229 (2011).
10. A. Valencia, G. Scarcelli, and Y. Shih, "Distant clock synchronization using entangled photon pairs," *Appl. Phys. Lett.* **85**, 2655–2657 (2004).
11. A. Valencia, M. V. Chekhova, A. Trifonov, and Y. Shih, "Entangled two-photon wave packet in a dispersive medium," *Phys. Rev. Lett.* **88**, 183601 (2002).
12. S.-Y. Baek, O. Kwon, and Y.-H. Kim, "Nonlocal dispersion control of a single-photon waveform," *Phys. Rev. A* **78**, 013816 (2008).
13. S.-Y. Baek, O. Kwon, and Y.-H. Kim, "Temporal shaping of a heralded single-photon wave packet," *Phys. Rev. A* **77**, 013829 (2008).

14. M. Avenhaus, A. Eckstein, P. J. Mosley, and C. Silberhorn, "Fiber-assisted single-photon spectrograph," *Opt. Lett.* **34**, 2873–2875 (2009).
15. A. Pe'er, B. Dayan, A. A. Friesem, and Y. Silberberg, "Temporal shaping of entangled photons," *Phys. Rev. Lett.* **94**, 073601 (2005).
16. B. Dayan, Y. Bromberg, I. Afek, and Y. Silberberg, "Spectral polarization and spectral phase control of time-energy entangled photons," *Phys. Rev. A* **75**, 043804 (2007).
17. F. Züh, M. Halder, and T. Feurer, "Amplitude and phase modulation of time-energy entangled two-photon states," *Opt. Express* **16**, 16452–16458 (2008).
18. C. Bernhard, B. Bessire, T. Feurer, and A. Stefanov, "Shaping frequency-entangled qudits," *Phys. Rev. A* **88**, 032322 (2013).
19. J. M. Lukens, A. Dezfouliyan, C. Langrock, M. M. Fejer, D. E. Leaird, and A. M. Weiner, "Biphoton manipulation with a fiber-based pulse shaper," *Opt. Lett.* **38**, 4652–4655 (2013).
20. J. M. Lukens, A. Dezfouliyan, C. Langrock, M. M. Fejer, D. E. Leaird, and A. M. Weiner, "Demonstration of high-order dispersion cancellation with an ultrahigh-efficiency sum-frequency correlator," *Phys. Rev. Lett.* **111**, 193603 (2013).
21. J. M. Lukens, A. Dezfouliyan, C. Langrock, M. M. Fejer, D. E. Leaird, and A. M. Weiner, "Orthogonal spectral coding of entangled photons," *Phys. Rev. Lett.* **112**, 133602 (2014).
22. Y. J. Lu, R. L. Campbell, and Z. Y. Ou, "Mode-locked two-photon states," *Phys. Rev. Lett.* **91**, 163602 (2003).
23. J. M. Lukens, O. Odele, C. Langrock, M. M. Fejer, D. E. Leaird, and A. M. Weiner, "Generation of biphoton correlation trains through spectral filtering," *Opt. Express* **22**, 9585–9596 (2014).
24. P. Kolchin, C. Belthangady, S. Du, G. Y. Yin, and S. E. Harris, "Electro-optic modulation of single photons," *Phys. Rev. Lett.* **101**, 103601 (2008).
25. C. Belthangady, S. Du, C.-S. Chuu, G. Y. Yin, and S. E. Harris, "Modulation and measurement of time-energy entangled photons," *Phys. Rev. A* **80**, 031803 (2009).
26. S. Sensarn, G. Y. Yin, and S. E. Harris, "Observation of nonlocal modulation with entangled photons," *Phys. Rev. Lett.* **103**, 163601 (2009).
27. C. Belthangady, C.-S. Chuu, I. A. Yu, G. Y. Yin, J. M. Kahn, and S. E. Harris, "Hiding single photons with spread spectrum technology," *Phys. Rev. Lett.* **104**, 223601 (2010).
28. C. Liu, Y. Sun, L. Zhao, S. Zhang, M. M. T. Loy, and S. Du, "Efficiently loading a single photon into a single-sided Fabry-Perot cavity," *Phys. Rev. Lett.* **113**, 133601 (2014).
29. J. van Howe and C. Xu, "Ultrafast optical signal processing based upon space-time dualities," *J. Lightwave Technol.* **24**, 2649 (2006).
30. V. Torres-Company, J. Lancis, and P. Andrés, "Space-time analogies in optics," in *Progress in Optics*, E. Wolf ed. (Elsevier, 2011), vol. 56, pp. 1–80.
31. J. van Howe and C. Xu, "Ultrafast optical delay line by use of a time-prism pair," *Opt. Lett.* **30**, 99–101 (2005).
32. J. Sharping, Y. Okawachi, J. van Howe, C. Xu, Y. Wang, A. Willner, and A. Gaeta, "All-optical, wavelength and bandwidth preserving, pulse delay based on parametric wavelength conversion and dispersion," *Opt. Express* **13**, 7872–7877 (2005).
33. Y. Wang, C. Yu, L. Yan, A. E. Willner, R. Roussev, C. Langrock, M. M. Fejer, J. E. Sharping, and A. L. Gaeta, "44-ns continuously tunable dispersionless optical delay element using a PPLN waveguide with two-pump configuration, DCF, and a dispersion compensator," *IEEE Photon. Technol. Lett.* **19**, 861–863 (2007).
34. J. D. Franson, "Nonlocal cancellation of dispersion," *Phys. Rev. A* **45**, 3126–3132 (1992).
35. S.-Y. Baek, Y.-W. Cho, and Y.-H. Kim, "Nonlocal dispersion cancellation using entangled photons," *Opt. Express* **17**, 19241–19252 (2009).
36. K. A. O'Donnell, "Observations of dispersion cancellation of entangled photon pairs," *Phys. Rev. Lett.* **106**, 063601 (2011).
37. Y. Shih, "Entangled biphoton source - property and preparation," *Rep. Prog. Phys.* **66**, 1009 (2003).
38. K. R. Parameswaran, R. K. Route, J. R. Kurz, R. V. Roussev, M. M. Fejer, and M. Fujimura, "Highly efficient second-harmonic generation in buried waveguides formed by annealed and reverse proton exchange in periodically poled lithium niobate," *Opt. Lett.* **27**, 179–181 (2002).
39. C. Langrock, S. Kumar, J. E. McGeehan, A. E. Willner, and M. M. Fejer, "All-optical signal processing using $\chi^{(2)}$ nonlinearities in guided-wave devices," *J. Lightwave Technol.* **24**, 2579–2592 (2006).
40. B. Dayan, "Theory of two-photon interactions with broadband down-converted light and entangled photons," *Phys. Rev. A* **76**, 043813 (2007).
41. R. Prevedel, K. M. Schreier, J. Lavoie, and K. J. Resch, "Classical analog for dispersion cancellation of entangled photons with local detection," *Phys. Rev. A* **84**, 051803 (2011).
42. O. Kuzucu, F. N. C. Wong, S. Kurimura, and S. Tovstonog, "Time-resolved single-photon detection by femtosecond upconversion," *Opt. Lett.* **33**, 2257–2259 (2008).
43. O. Kuzucu, F. N. C. Wong, S. Kurimura, and S. Tovstonog, "Joint temporal density measurements for two-photon state characterization," *Phys. Rev. Lett.* **101**, 153602 (2008).
44. M. Asobe, O. Tadanaga, H. Miyazawa, Y. Nishida, and H. Suzuki, "Multiple quasi-phase-matched LiNbO₃ wave-length converter with a continuously phase-modulated domain structure," *Opt. Lett.* **28**, 558–560 (2003).

45. J. van Howe and C. Xu, "Ultrafast optical delay line using soliton propagation between a time-prism pair," *Opt. Express* **13**, 1138–1143 (2005).
 46. T.-J. Ahn, Y. Park, and J. Azaña, "Fast and accurate group delay ripple measurement technique for ultralong chirped fiber Bragg gratings," *Opt. Lett.* **32**, 2674–2676 (2007).
 47. P. Kumar, "Quantum frequency conversion," *Opt. Lett.* **15**, 1476–1478 (1990).
-

1. Introduction

Entangled quantum-optical states offer unique potential in a range of applications, from secure communications [1, 2] and high-speed computing [3, 4] to quantum teleportation [5–7] and enhanced metrology [8, 9]. The stronger-than-classical correlations shared by such entangled modes or quanta can be exploited to realize capabilities unattainable with classical fields. For example, the temporal correlation of frequency-entangled, photon-number-squeezed states can yield significant enhancements in positioning schemes based on timing measurements [8]. And the tendency of entangled photon pairs (or "biphotons") to be detected in coincidence—even though individual arrival times are random—has been used directly to synchronize distant clocks with high precision [10]. These examples emphasize the value of exploiting the intrinsic spectro-temporal correlations of entangled states, and recent years have witnessed a substantial interest in not only *utilizing* such entanglement, but also *manipulating* it with optical signal-processing techniques, particularly in the context of entangled photon pairs. Some areas that have been explored include propagation through dispersive media [11–14], Fourier-transform pulse shaping [15–21], generation of comblike correlations [22, 23] and biphoton electro-optic modulation [24–28]. However, reconfigurable control of relative photon delays—of relevance in applications based on biphoton timing measurements—has yet to receive the same attention. Accordingly, here we consider a novel manipulation scheme in which we are able to tune the relative arrival times of the biphotons by simply shifting the pump frequency, making use of nonlocal dispersion cancellation for low-distortion performance.

In classical photonics, tunable delay systems are used in a variety of applications, including metrology and communications [29, 30]. In its most basic form, delay control can be realized by varying the optical path length traversed by the field through the system. Unfortunately, the switching speed of this approach is limited to the \sim kHz range by the mechanical motion of a delay stage or mirror. Alternatively, drastically faster modulation is possible through a setup using wavelength conversion followed by dispersion [31]. Since different frequencies propagate at distinct group velocities through a dispersive medium, the amount of wavelength shift applied to the input field (either through electro-optic modulation or nonlinear mixing) maps directly to the delay of the output; thus, by tuning the frequency shift, it is possible to modulate the applied delay, in some cases with GHz switching speeds [29]. However, this delay comes at a price: dispersion not only shifts the arrival time, but also causes the pulse to spread. Therefore compensation is typically achieved by propagating through equal and opposite group velocity dispersion before shifting the original wavelength or after shifting the output wavelength back to its original value [31–33]. Figure 1(a) depicts a standard setup for classical tunable delay control.

Building on these classical systems, here we propose and demonstrate tunable delay control of nonclassical time-frequency entangled photons for the first time, through shifting the pump frequency and propagating the generated biphotons through optical dispersion. In related past experiments [12, 13], the frequency-dependent group delay of dispersive fiber was combined with spectral filtering to modify the arrival time of heralded single photons. Yet such passive filtering not only eliminates large fractions of the photon flux but, by reducing the total bandwidth, also lengthens the bandlimited correlation time, an undesirable consequence especially relevant to experiments resolving ultrafast correlations. Here we instead consider pump-

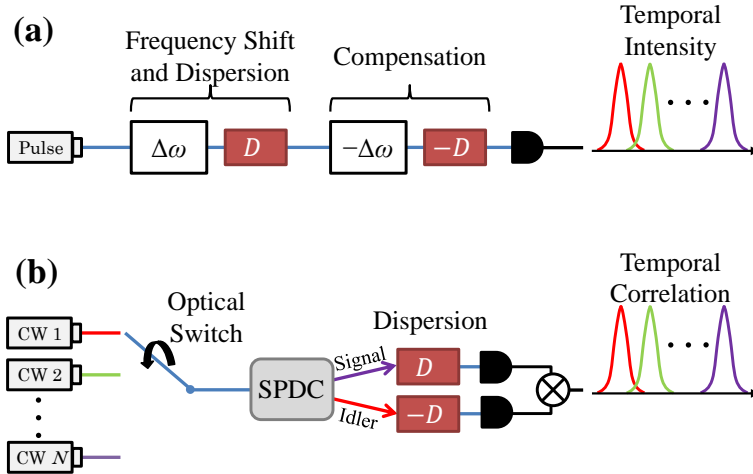


Fig. 1. (a) Classical delay control scheme based on wavelength conversion and dispersion. (b) General scheme for delay control of time-frequency entangled photons through pump frequency tuning and propagation in dispersive media.

frequency modulation, a previously underutilized degree of freedom in biphoton manipulation experiments offering the potential advantages of rapid delay tuning and the ability to shift the delay of nearly the full biphoton spectrum. Temporal spreading is minimized in our proposed scheme by exploiting nonlocal dispersion cancellation—an effect whereby applying equal and opposite dispersion to the signal and idler photons leaves the biphoton correlation function unaltered [20, 34–36]. This allows us to compensate for the broadening which would otherwise degrade the sharpness of the temporal correlations. A schematic for this tunable delay control is shown in Fig. 1(b). We note that this new method for entangled photon control represents a quantum-optical analogue of classical pulse-position modulation. Our delay control method can be applied for obtaining a wide range of delays, but we focus on picosecond-scale control in these experiments.

2. Theory

The probability of detecting the signal photon delayed by some time τ with respect to the idler is specified by the second-order correlation function $G^{(2)}(\tau)$, which is equivalent to the square modulus of the two-photon wavepacket $\psi(\tau)$ [37]:

$$\psi(\tau) = \langle \text{vac} | \hat{E}_i^{(+)}(t) \hat{E}_s^{(+)}(t + \tau) | \Psi \rangle, \quad (1)$$

where $|\Psi\rangle$ is the state generated from spontaneous parametric down conversion (SPDC), $|\text{vac}\rangle$ denotes the vacuum state, and $\hat{E}_{s,i}^{(+)}$ are the positive-frequency field operators for the signal and idler photons, respectively. For biphotons obtained through SPDC of a monochromatic pump laser and propagating through linear and time-invariant systems, the output wavepacket can be expressed as [20]

$$\psi(\tau) \propto \int d\Omega \phi(\Omega) H_s(\omega_0 + \Omega) H_i(\omega_0 - \Omega) e^{-i\Omega\tau}, \quad (2)$$

where $\phi(\Omega)$ represents the biphoton spectrum, $H_s(\omega)$ and $H_i(\omega)$ are the complex transfer functions applied to the signal and idler, respectively, and ω_0 is the center frequency of the biphoton spectrum, one-half that of the single-frequency pump. Furthermore, if the spectral filters H_s and H_i are pure-phase and antisymmetric with respect to each other, dispersion cancellation

(net zero spectral phase) can be achieved [20, 34]. Hence, if we apply second-order dispersion to the biphotons by setting $H_s(\omega) = \exp[iA_s(\omega - \omega_0)^2/2]$ and $H_i(\omega) = \exp[iA_i(\omega - \omega_0)^2/2]$, then there will be cancellation [$H_s(\omega_0 + \Omega)H_i(\omega_0 - \Omega) = 1$] when $A_s = -A_i = A$. In this case, Eq. (2) can now be written as

$$\psi(\tau) \propto \int d\Omega \phi(\Omega) e^{-i\Omega\tau}, \quad (3)$$

as if the biphoton never experienced any dispersion.

Yet as examined in [20], opposite signs of dispersion give cancellation only for even spectral phase orders; for odd orders, opposite signs add cumulatively. This implies an important distinction between delay (first-order spectral phase) and second-order dispersion, for if we detune the center frequency of the biphotons relative to the quadratic dispersion by $\delta\omega$ such that $\omega'_0 = \omega_0 + \delta\omega$ is the new center frequency, the fixed filters H_s and H_i now introduce additional phase terms linear in frequency, which because of the opposite signs of the coefficients ($A_s = -A_i$), *add* rather than cancel. Specifically, $H_s(\omega'_0 + \Omega)H_i(\omega'_0 - \Omega) = \exp(i2A\Omega\delta\omega)$ and the biphoton wavepacket is of the form

$$\psi(\tau) \propto \int d\Omega \phi(\Omega) e^{-i\Omega(\tau - 2A\delta\omega)}. \quad (4)$$

By the time-shift Fourier transform property, the phase term $\exp(i2A\Omega\delta\omega)$ corresponds to a temporal delay of $2A\delta\omega$, directly proportional to both the strength of the dispersion and magnitude of the frequency tuning. In this way the delays imparted by the signal and idler dispersive media are retained, while the associated wavepacket spreading is removed, a fortuitous situation made possible by the spectral anticorrelation of the entangled state. Such a finding indicates that by shifting the pump laser frequency, one can modulate the relative arrival times of entangled photons with minimal impact on the shape of their correlation. In contrast to tunable optical delay lines requiring mechanical adjustment, the filters here are fixed, so that our scheme could in principle be implemented rapidly by simply switching between pump lasers along a fixed frequency grid.

3. Experiments

Our experimental setup is depicted in Fig. 2. We generate entangled photons through degenerate SPDC by pumping a 67-mm-long periodically poled lithium niobate (PPLN) waveguide [38,39] with a continuous-wave (CW) laser (New Focus TLB-6712). Residue pump photons are filtered out and the biphotons are fiber-coupled into a programmable pulse shaper (Finisar WaveShaper 1000S), where the antisymmetric quadratic spectral phase, i.e., dispersion, is applied to the biphoton spectrum—the signal (idler) photon is defined to have frequency greater (less) than one-half that of the pump. The pulse shaper here gives us access to the biphoton spectrum in the frequency range from 191.250 to 196.275 THz with a resolution of 10 GHz. It also applies additional phase to compensate for the dispersion from the optical fibers connecting the collimators to the pulse shaper. Another PPLN waveguide, the phase-matching peak of which is aligned with the first waveguide through temperature control, is then used to perform sum-frequency generation (SFG) on the spectrally shaped biphotons. Unlike correlation measurements with two single-photon detectors, SFG permits direct measurement of the temporal correlations with a single detector and on an ultrafast timescale [15,40], necessary to resolve the picosecond delay shifts in this experiment. After filtering out the unconverted biphotons, we detect the SFG photons on a silicon single-photon avalanche photodiode (PicoQuant τ -SPAD). The second-order correlation function $G^{(2)}(\tau) = |\psi(\tau)|^2$ can then be measured by sweeping additional linear spectral-phase terms on the pulse shaper and recording the SFG rate at each step [15,20]. Since we send both photons through the same fiber and recombine them via SFG for detection, this

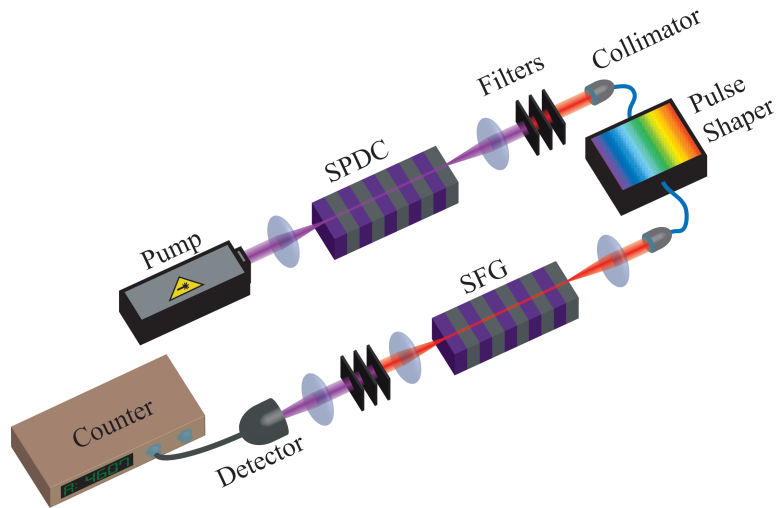


Fig. 2. Experimental setup. Pump photons decay into signal and idler photons in a PPLN waveguide. The pulse shaper is used to apply antisymmetric dispersion to the filtered signal and idler photons, and then they recombine in another PPLN waveguide through SFG. The coincidence rate is measured using a single-photon counter while the delay steps are determined by applying linear spectral phase on the pulse shaper.

proof-of-concept experiment is in some sense “local,” rather than an example of truly nonlocal dispersion cancellation. However, whereas background-free classical analogues of dispersion cancellation [41] *require* local nonlinear detection to realize the effect, in our case we use SFG only as a *tool* to achieve the necessary subpicosecond timing resolution. Thus the proposed concept applies just as well to truly nonlocal systems such as the schematic in Fig. 1(b); realizing this experimentally would require either significantly larger amounts of dispersion or ultrafast nonlocal detection, e.g., with classical-pulse-assisted upconversion [42, 43]. So while the results below clearly demonstrate the fundamental effect, a nonlocal experiment does represent an important direction for future work.

In the proposed arrangement above, we assume fixed dispersion and a tunable pump laser; this is most compatible with previous classical approaches and rapid switching capabilities. Yet the basic physics is based only on modulation of the *relative* frequency spacing between the dispersion and the SPDC center frequency, so in our first demonstration, the dispersion profile on the pulse shaper is shifted relative to a fixed pump frequency, as shown in Fig. 3(a). In this case, we do not require a nonlinear medium phase-matched for SPDC at multiple pump wavelengths, and so we can employ a PPLN waveguide with a uniform poling pattern to give maximum efficiency, generating biphotons with a center wavelength of 1547.20 nm (193.9 THz). Figure 3(b) shows the phase-matching curve of this PPLN waveguide (measured second-harmonic-generation conversion efficiency as a function of pump frequency and normalized to the input power [38]). From this measurement, we glean that pump wavelengths in a narrow band around 773.6 nm should be phase-matched for parametric downconversion. We mention, though, that the bandwidth of the generated biphotons—i.e., the spectral width of $\phi(\Omega)$ —is much wider than that of the curve in Fig. 3(b), since the signal and idler fields need not have the same frequency, only a fixed sum. Accordingly, an accurate classical measure of the SPDC bandwidth is instead that of difference-frequency mixing [39]. Specifically, the total bandwidth in our experiment is on the order of that found in [20], essentially flat over the 5-THz pulse-shaper passband.

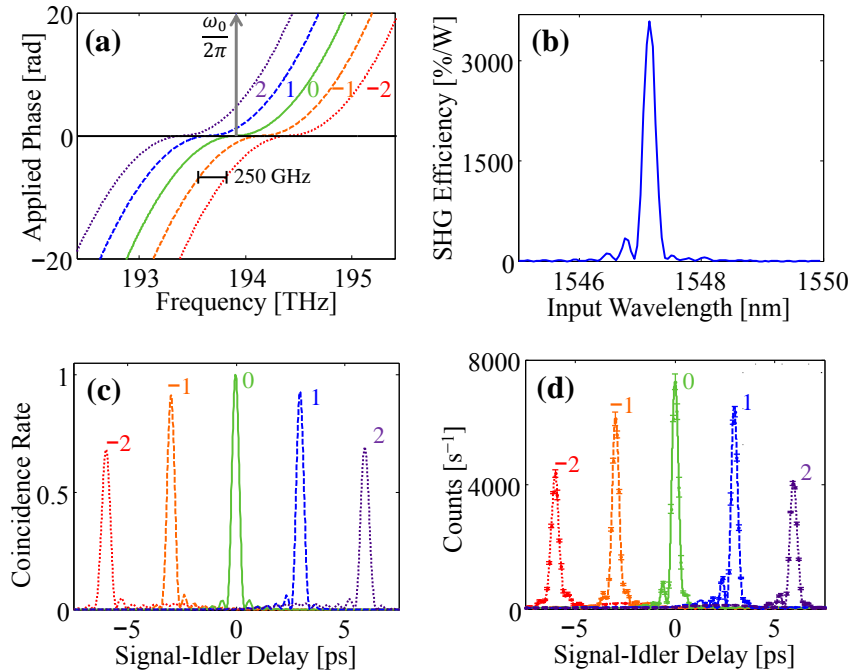


Fig. 3. Experiments with fixed pump. (a) Schematic of a fixed pump with shifts in the antisymmetric dispersion curve displayed over 3 THz of the 5 THz pulse shaper window. (b) Phase-matching curve for PPLN waveguide with a uniform poling pattern. (c) Theoretical and (d) experimental results showing delay control of the biphoton correlation function. The numbers $[-2 -1 0 1 2]$ correspond to the amount the dispersion curve is shifted in each case, in units of 250 GHz.

Setting the dispersion constant at $A = 3/\pi \text{ ps}^2$ and the center of the antisymmetric quadratic dispersion curve (zero-crossing) at 193.9 THz, we measure a single correlation peak around zero delay as expected for perfect dispersion cancellation [peak labeled “0” in Fig. 3(d)]. Subsequently, when we move the center of the antisymmetric curve by integer multiples of 250 GHz, we obtain the results shown in Fig. 3(d)—temporal delays of -6 , -3 , 3 , and 6 ps are measured for -500 , -250 , 250 , and 500 GHz shifts in the center of the antisymmetric curve, respectively. Our experimental results [Fig. 3(d)] are in excellent agreement with theory [Fig. 3(c)]. We point out that the reduction in the peak number of counts for our delayed correlations is a consequence of designating our signal and idler photons by frequency. Thus, when we shift the antisymmetric dispersion, there is a portion of the biphoton spectrum (in a $2\delta\omega$ -wide bandwidth) where the signal and idler photons both experience the same sign of dispersion. The result of this uncompensated dispersion is evident in tails that develop in the shifted correlations, particularly visible in the two exterior curves in Figs. 3(c) and 3(d). Nonetheless, the displaced peaks themselves show minimal temporal spreading, confirming our ability to shift and compensate nearly the entire biphoton. Moreover, we emphasize that these nonidealities stem only from the nature of the entangled photons here, which can only be distinguished by frequency, and is not inherent to the method itself. For example, in situations where it is possible to spatially separate signal and idler for all pump frequencies (e.g., in noncollinear or type-II downconversion), one could ensure that the entire spectrum of each photon sees the desired dispersion, giving perfect cancellation—in terms of both width and shape—at all delay shifts.

We now move on to our main demonstration of biphoton tunable delay: by tuning the pump

frequency relative to a fixed antisymmetric dispersion profile. PPLN waveguides with uniform quasi-phase-matched (QPM) patterns offer exceptionally high conversion efficiency but, for lengths of several centimeters, accept only a small range of pump wavelengths (~ 0.1 nm) for phase-matched down-conversion. So in order to permit a series of discrete pump frequencies with wider separations, we fabricate a QPM grating with a phase-modulated poling pattern designed to give roughly equal down-conversion efficiency and bandwidth at five distinct pump wavelengths [44]. Figure 4(b) shows the measured SHG phase-matching curve of this grating, suggesting comparable down-converted power at each frequency. Therefore, we replace the uniformly poled lithium niobate waveguides in our setup with ones that have such a modulated poling pattern. Our pump wavelength is set to 774 nm (193.8 THz), corresponding to the middle peak of the phase-matching curve, in order to generate biphotons with a center wavelength at 1548 nm, and we position the center of the antisymmetric quadratic dispersion to match this wavelength with $A = 3/\pi$ ps². As anticipated, there is a sharp correlation peak at zero delay due to dispersion cancellation [Fig. 4(d)]. Detuning the wavelength of our laser by 2, 1, -1 , and -2 nm—giving rise to -500 , -250 , 250, and 500 GHz shifts in the biphoton center frequency—we are able to measure correlation functions with single peaks around -6 , -3 , 3, and 6 ps, respectively, as shown in Fig. 4(d). Again, our experimental results [Fig. 4(d)] are in very good agreement with theory [Fig. 4(c)], confirming the robustness of our scheme. The total count rate is reduced by a factor of about 10 compared to the results of Fig. 3(d) due to the reduced efficiency of the phase-modulated waveguides. We also note that there is an additional drop in the relative peak amplitude for our delayed correlations in this demonstration compared to the first. Recall that our pulse shaper can only access frequencies between 191.250 and 196.725 THz and hence, as we move the center frequency of the biphotons, we decrease the fraction of the biphoton spectrum transmitted through the pulse shaper—an effect also included in simulation to obtain Fig. 4(c). This explains the additional reduction in the delayed coincidence counts, over and above that caused by biphotons that experience the same sign of dispersion (mentioned earlier).

So far, we have shown results for biphoton delay tuning up to ± 6 ps using our experimental setup. We now analyze the performance of our system with respect to metrics that help us examine the extent of the delays we can achieve using our setup. One metric we consider is the fractional delay: the ratio of the delay of the correlation peak to the FWHM of the zero-delay correlation function. We adopt this from the figure of merit used in classical delay lines where one measures the ratio of the delay of the output pulse to the input pulse width [45]. Another metric we include is the normalized peak number of counts, which gives us an idea of the fraction of the biphotons successfully shifted in delay, hence some information about the distortion in our scheme. In the case of the fixed pump with shifts in the dispersion profile, the measured correlation peaks for ± 250 and ± 500 GHz shifts correspond to fractional delays of ± 7.5 (normalized peak count rate at 87%) and ± 15 (normalized peak count rate at 58%), respectively, while in the case of a fixed dispersion profile with shifts in the pump frequency, we obtain fractional delays of ± 7.5 and ± 15 with normalized peak count rates at 73% and 38%, respectively. These results are approximately confirmed by simulation (Fig. 5)—we emphasize that our simulation results account for the segments of the biphoton spectrum that experience the same sign of dispersion and the finite bandwidth of our pulse shaper, both of which contribute to reduced count rates for delayed correlations. Moreover the amount of dispersion we can apply is limited by the finite resolution of our pulse shaper. Based on previous tests with this device [23], we anticipate maximum delay shifts up to around ± 30 ps should be possible.

Looking forward, much longer delays can be achieved with dispersive elements possessing significantly larger values of the constant A . Ultimately, the fundamental constraints to this delay scheme are imposed by a combination of the pump and biphoton source—dispersion

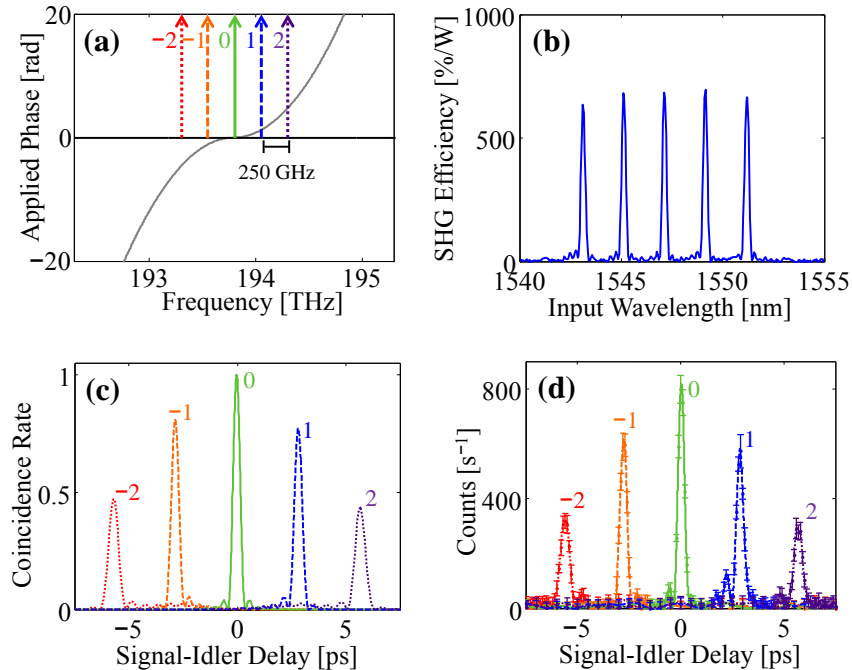


Fig. 4. Experiments with fixed dispersion. (a) Schematic of a fixed antisymmetric dispersion curve with shifts in pump frequency displayed over 3 THz of the 5 THz pulse shaper window. (b) Phase-matching curve for PPLN waveguide with a non-uniform poling pattern. (c) Theoretical and (d) experimental results showing delay control of the biphoton correlation function. The numbers $[-2 -1 0 1 2]$ correspond to the amount the center frequency of the biphoton is shifted in each case, in units of 250 GHz.

cancellation can only be accomplished for group delay spreading less than the pump coherence time (on the order of a microsecond for our pump linewidth of ~ 200 kHz), while the phase matching acceptance bandwidth of the biphoton source determines the allowable center frequency shifts. Practically though, propagation loss in the dispersive media would likely be more limiting, and thus, a chirped fiber Bragg grating (CFBG) would be preferred over optical fibers for obtaining large delay shifts. For example, a commercial CFBG [46] with an 80-ns dispersion-bandwidth product and a 3-dB insertion loss would allow delay shifts easily resolvable with electronic coincidence detection. By comparison, the equivalent length of Corning SMF-28e fiber would attenuate the optical signal by about 24 dB. We also reiterate that spatial rather than spectral separation of the signal-idler photons would eliminate the temporal distortion of the shifted peaks obtained in this experiment. Combined with a pure dispersive medium in which higher order phase is either negligible or compensated, such separation will potentially allow us to demonstrate longer delays without appreciable spreading. Finally we note that the arrangement considered here permanently shifts the biphoton center frequency, creating a one-to-one correspondence between the delay shift and center wavelength. Yet in analogy to the classical scheme in Fig. 1(a), the time-shifted biphoton in all cases can be returned to the same center wavelength through quantum frequency conversion [47].

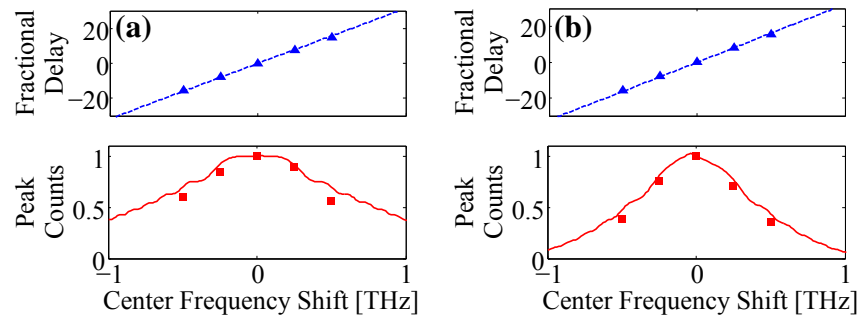


Fig. 5. Fractional delay and normalized peak count rate vs. shift in center frequency for (a) the case of a fixed pump with shifts in the antisymmetric dispersion curve and (b) the case of a fixed antisymmetric dispersion curve and shifts in pump frequency. The markers denote experimental results; the curves, simulation.

4. Conclusion

We have described and demonstrated a new way to tune the temporal position of the second-order correlation function for entangled photons. By shifting the frequency of the pump and applying dispersion cancellation, we can control the relative delay of the signal-idler photons without introducing significant distortion. We believe that our scheme will be useful for delay correction in time-energy quantum key distribution systems. In future experiments, elements such as optical fibers and CFBGs can provide the necessary dispersion, replacing the pulse shaper in this scheme, and could in principle introduce much longer delays that are resolvable with electronic coincidence detection. Finally, it will be interesting to explore some other capabilities with this technique such as rapidly modulating the pump frequency and encoding the pump frequency with binary information.

Acknowledgments

This work was funded by the National Science Foundation under grant ECCS-1407620 and by the Office of Naval Research under Grant No. N000141210488. J. M. L. acknowledges financial support from the Department of Defense through a National Defense Science and Engineering Graduate Fellowship. J. A. J. acknowledges support from Colciencias Colombia through the Francisco Jose de Caldas Conv. 529 scholarship and Fulbright Colombia.